Non-LTE Line Transfer with Diffusion of Excited Atoms II

D. F. Düchs, S. Rehker

Max-Planck-Institut für Plasmaphysik, D-8046 Garching bei München, F.R. Germany
Euratom-Assoziation

and J. Oxenius

Faculté des Sciences, Université Libre de Bruxelles, B-1050 Brussels, Belgium
Association Euratom-Etat Belge

Z. Naturforsch. **33a**, 124—129 (1978); received December 5, 1977

Non-LTE radiative transfer in a spectral line due to two-level atoms is studied taking the diffusion of excited atoms into account. Numerical results are presented for the case of a stationary, plane parallel plasma of constant total density and temperature without external radiation and without exchange of matter with the surroundings, assuming pure Doppler broadening of the spectral line.

1. Introduction

In the first part of this paper [1] (in the following referred to as Part I) we have pointed out that in optically thick non-LTE plasmas (where LTE stands for "local thermodynamic equilibrium"), radiative transfer in spectral lines gives rise to density gradients and thus to diffusion currents of excited atoms even if the plasma is "homogeneous". As an illustrative example, we have considered the stationary radiation transport in a spectral line due to two-level atoms in a homogeneous and isothermal plasma of low temperature ($kT \ll h\nu_0$). Assuming complete redistribution, we have derived the equations that govern the formation of the spectral line if diffusion of excited atoms is taken into account. More specifically, for a plane parallel plasma without external radiation and without exchange of matter with the surroundings, the line source function obeys an integro-differential equation with appropriate boundary conditions [Part I, Eqs. (36)—(38)].

In this second part of the paper, we present numerical solutions of this integro-differential equation corresponding to typical non-LTE plasmas of large optical thickness, assuming that the line broadening is pure Doppler broadening. We have calculated the source function as a function of optical depth, the shape of the emergent spectral line, and the radiative energy loss of the plasma due to the emitted spectral line.

2. Equations

It is useful to introduce dimensionless quantities. We define the dimensionless frequency

$$x = (\nu - \nu_0)/\Delta\nu_D \tag{1}$$

which measures the frequency from the line center ν_0 in units of the Doppler width

$$\Delta\nu_D = (\nu_0/c)\,(2\,k\,T/m)^{1/2}\,, \tag{2}$$

m being the mass of a two-level atom. The line absorption coefficient [Part I, Eq. (5)] will be written

$$\varkappa_\nu = \varkappa\,\varphi_x\,, \tag{3}$$

where

$$\varkappa = (h\,\nu_0/4\,\pi)\,n_0\,B_{12}/\Delta\nu_D \tag{4}$$

has the dimension of an absorption coefficient. As we assume pure Doppler broadening, the dimensionless absorption profile $\varphi_x = \Delta\nu_D\,\varphi_\nu$ is given by

$$\varphi_x = \pi^{-1/2}\,e^{-x^2}; \quad \int_{-\infty}^{\infty}\varphi_x\,dx = 1\,. \tag{5}$$

The quantity $\varkappa$ is then related to the absorption coefficient in the line center, $\varkappa_0$, through $\varkappa = \pi^{1/2}\varkappa_0$. We define the optical depht τ in the plane parallel slab of geometrical thickness z^0 (Part I, Fig. 1) by means of $\varkappa$,

$$\tau = \varkappa(z^0 - z)\,, \tag{6}$$

choosing, as usual, the direction of the τ-scale opposite to that of the z-scale. We call the quantity

$$\tau^0 = \varkappa z^0 \tag{7}$$

the optical thickness of the slab. Finally, we define the dimensionless source function by

$$s(\tau) = S(z)/B^W\,, \tag{8}$$

and the dimensionless specific intensity by

$$i_x(\tau, \vartheta) = I_\nu(z, \vartheta)/B^W\,, \tag{9}$$

Reprint requests to Dr. J. Oxenius, Service de Chimie Physique II, Code Postal n° 231, Campus Plaine U.L.B., Boulevard du Triomphe, B-1050 Bruxelles.

where B^{W} is the Planck-Wien function [Part I, Eq. (15)].

In terms of these dimensionless quantities, the integro-differential equation for the source function [Part I, Eqs. (36) and (37)] can be written

$$s(\tau) - \delta_0 s''(\tau) = \varepsilon_0 + (1-\varepsilon_0)\int_0^{\tau^0} K_1(|\tau-\tau'|)\, s(\tau')\,\mathrm{d}\tau' \quad (10)$$

with the kernel function, defined for $\tau \geqq 0$,

$$K_1(\tau) = \tfrac{1}{2}\int_{-\infty}^{\infty} \varphi_x^2\, E_1(\varphi_x \tau)\,\mathrm{d}x\,, \quad (11)$$

$E_1(u)$ being the first exponential integral [Part I, Eq. (35)], and the boundary conditions [Part I, Eq. (38)] are

$$s'(0) = s'(\tau^0) = 0\,. \quad (12)$$

Here $s'(\tau) = \mathrm{d}s/\mathrm{d}\tau$ and $s''(\tau) = \mathrm{d}^2 s/\mathrm{d}\tau^2$.

Apart from the optical thickness of the slab, τ^0, two dimensionless parameters appear in the integro-differential equation (10): the collision parameter ε_0 and the diffusion parameter δ_0. They are given explicitly by

$$\varepsilon_0 = \varepsilon/(1+\varepsilon)\,, \quad (13)$$

$$\delta_0 = (\varkappa^2 D/A_{21})/(1+\varepsilon)\,. \quad (14)$$

Here, $\varepsilon = n_{\mathrm{e}} C_{21}/A_{21}$ [Part I, Eq. (19)] is the ratio of the frequencies of electronic de-excitation collisions and of spontaneous emissions, and D is the diffusion constant. Clearly,

$$0 < \varepsilon_0 < 1 \quad \text{and} \quad 0 < \delta_0 < \infty\,.$$

We recall that, in our case, gradients of excited atoms occur only in non-LTE plasmas ($\varepsilon \ll 1$) of large optical thickness ($\tau^0 \gg 1$). On the other hand, in optically thin plasmas ($\tau^0 \ll 1$), the source function is given by $s = \varepsilon_0$, while in LTE plasmas ($\varepsilon \gg 1$) it is given by the Planck function, $s = 1$, for any optical thickness. Obviously, Eq. (10) need not be considered in either case. If both $\varepsilon_0 \ll 1$ and $\tau^0 \gg 1$ hold, there is true non-LTE radiative transfer giving rise to gradients of excited atoms, and the diffusion parameter δ_0 is then a measure of whether diffusion of excited atoms is important ($\delta_0 \gtrsim 1$) or not ($\delta_0 \ll 1$). Up to now, only the limiting case of vanishing diffusion ($\delta_0 = 0$) has been treated in the literature on non-LTE line transfer.

Once the source function $s(\tau)$ is known, all spectroscopic properties of the system can easily be deduced from it. For example, the specific intensity $i_x(0, \vartheta)$ emerging from the boundary $\tau = 0$ in a direction specified by the angle ϑ with respect to the normal of the plane, with $0 \leqq \vartheta < \pi/2$, is given by

$$i_x(0,\vartheta) = \varphi_x \int_0^{\tau^0} s(\tau)\exp(-\varphi_x \tau/\cos\vartheta)\,\mathrm{d}\tau/\cos\vartheta\,. \quad (15)$$

In particular, the intensity emitted in the direction perpendicular to the boundary plane is

$$i_x^{\mathrm{out}} = \varphi_x \int_0^{\tau^0} s(\tau)\exp(-\varphi_x\tau)\,\mathrm{d}\tau\,. \quad (16)$$

Let

$$w = \int_{-\infty}^{\infty} w_x\,\mathrm{d}x \quad (17)$$

be the total radiative energy loss (in units of the Planck-Wien function) per unit time and unit area due to the considered spectral line. One has

$$w_x = \int_0^{\pi/2} i_x(0,\vartheta)\cos\vartheta\, 2\pi\sin\vartheta\,\mathrm{d}\vartheta\,. \quad (18)$$

Inserting here Eq. (15), one obtains after a simple change of the integration variable

$$w_x = 2\pi\varphi_x \int_0^{\tau^0} s(\tau)\, E_2(\varphi_x\tau)\,\mathrm{d}\tau \quad (19)$$

where

$$E_2(u) = \int_1^{\infty} (e^{-ut}/t^2)\,\mathrm{d}t \quad (20)$$

is the second exponential integral. The total radiative energy loss, Eq. (17), is thus

$$w = 2\pi \int_0^{\tau^0} K_2(\tau)\, s(\tau)\,\mathrm{d}\tau \quad (21)$$

with the kernel function

$$K_2(\tau) = \int_{-\infty}^{\infty} \varphi_x E_2(\varphi_x\tau)\,\mathrm{d}x\,, \quad (22)$$

defined for $\tau \geqq 0$. More instructive from a physical point of view than the quantity w itself is the ratio

$$\eta = w/w^{\mathrm{LTE}} \quad (23)$$

where w^{LTE} denotes the corresponding energy loss in LTE, which is obtained from Eq. (21) for $s(\tau) \equiv 1$.

3. Numerical Results and Discussion

We have solved numerically the integro-differential equation (10) for two typical non-LTE plasmas, characterized by $\varepsilon_0 = 10^{-2}$ and 10^{-4}, respectively, and various combinations of τ^0 and δ_0. The numerical method used is described in the Appendix.

Concerning our choice of optical thicknesses τ^0, we must first recall the following distinction between two types of isothermal, optically thick plasmas [2]: For a given spectral line, an optically thick plasma is called "effectively thick" if, in its interior, the line source function approaches the value of the Planck function. In contrast, an optically thick plasma is called "effectively thin" if nowhere in its interior does the line source function approache the value of the Planck function. Our choice of optical thicknesses was therefore such that diffusion effects could be studied both in effectively thin and effectively thick systems. For the case of pure Doppler broadening it has been shown by numerical calculations [2] that, for two-level atoms and vanishing diffusion, a plane parallel slab is effectively thick if its optical thickness obeys $\tau^0 \gtrsim 10\,\varepsilon_0^{-1}$.

On the other hand, the diffusion parameters chosen by us cover a range from weak ($\delta_0 \ll 1$) to strong ($\delta_0 \gg 1$) diffusion. In addition, we have calculated the diffusion-free limiting case ($\delta_0 = 0$) for comparison.

Explicitly, we have chosen the following set of parameters for studying the effects of diffusion of excited atoms:

$$\varepsilon_0 = 10^{-2}: \quad \tau^0 = 10\ ;\ 10^2;\ 10^3\,.$$

$$\varepsilon_0 = 10^{-4}: \quad \tau^0 = 10^2;\ 10^4;\ 10^6\,.$$

Here the smallest values of τ^0 refer to effectively thin systems, the intermediate ones to almost effectively thick systems, and the largest ones to effectively thick systems. For each pair of parameters ε_0, τ^0, the following values of δ_0 were considered:

$$\delta_0 = 0;\ 0.01;\ 0.1;\ 1;\ 10;\ 100\,.$$

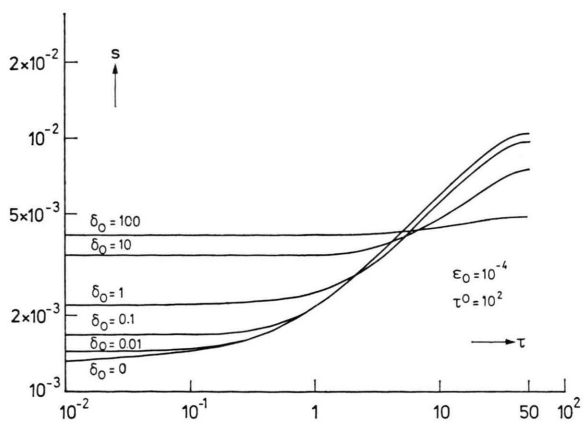

Fig. 1. The dimensionless source function s as a function of optical depth τ. The source function s is symmetric about the center of the plane parallel slab, $\tau = \frac{1}{2}\tau^0$. The cases shown correspond to effectively thin systems.

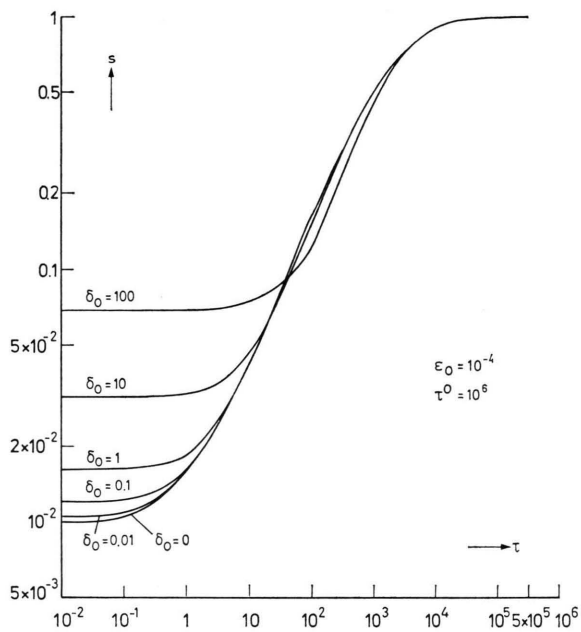

Fig. 2. The dimensionless source function s as a function of optical depth τ. The source function s is symmetric about the center of the plane parallel slab, $\tau = \frac{1}{2}\tau^0$. The cases shown correspond to effectively thick systems.

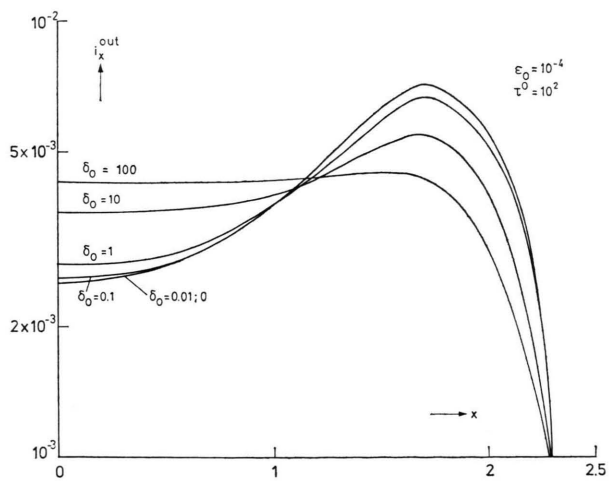

Fig. 3. The dimensionless specific intensity i_x^{out} emerging in the direction perpendicular to the boundary plane, as a function of the dimensionless frequency x. The intensity i_x^{out} is symmetric about the line center $x = 0$. The cases shown correspond to the effectively thin systems in Figure 1.

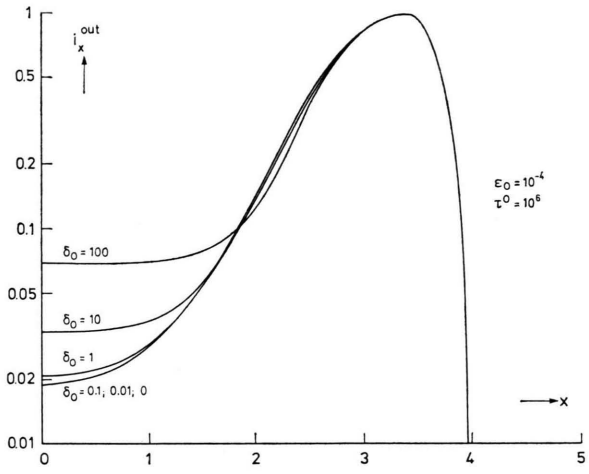

Fig. 4. The dimensionless specific intensity i_x^{out} emerging in the direction perpendicular to the boundary plane, as a function of the dimensionless frequency x. The intensity i_x^{out} is symmetric about the line center $x = 0$. The cases shown correspond to the effectively thick systems in Figure 2.

The main results of our calculations are summarized in Figs. 1—4 and in Tables 1—3. Regarding Figs. 1 and 2, which show typical source functions corresponding to effectively thin and effectively thick systems, respectively, one should remember that the source function is proportional to the number density of excited atoms [Part I, Eq. (6)]

Tables 1. The total radiative energy loss η [Eq. (23)] and the source function at the boundary, $s_b = s(0) = s(\tau^0)$, and at the center, $s_c = s(\frac{1}{2}\tau^0)$, of the plane parallel slab. Read: $5.9^{-2} = 5.9 \times 10^{-2}$.

	$\varepsilon_0 = 10^{-2}$					
τ^0	δ_0	η	s_b	s_c	$\frac{s_c - s_b}{s_c + s_b}$	$\frac{s_c}{s_b}$
10	0	5.9^{-2}	3.5^{-2}	7.7^{-2}	0.38	2.2
	0.01	5.9^{-2}	3.8^{-2}	7.6^{-2}	0.34	2.0
	0.1	5.9^{-2}	4.2^{-2}	7.5^{-2}	0.28	1.8
	1	5.7^{-2}	4.8^{-2}	6.7^{-2}	0.16	1.4
	10	5.8^{-2}	5.7^{-2}	6.0^{-2}	0.03	1.1
	100	5.9^{-2}	5.8^{-2}	5.9^{-2}	0.00	1.0
10^2	0	0.26	8.3^{-2}	0.54	0.73	6.5
	0.01	0.26	9.1^{-2}	0.54	0.71	5.9
	0.1	0.26	0.11	0.54	0.67	5.1
	1	0.26	0.14	0.53	0.58	3.7
	10	0.28	0.22	0.46	0.35	2.1
	100	0.30	0.29	0.34	0.08	1.2
10^3	0	0.42	0.10	0.96	0.81	9.7
	0.01	0.42	0.11	0.96	0.80	8.8
	0.1	0.42	0.12	0.95	0.77	7.8
	1	0.43	0.17	0.96	0.70	5.7
	10	0.47	0.28	0.96	0.55	3.4
	100	0.58	0.48	0.94	0.32	2.0

Table 2. The total radiative energy loss η [Eq. (23)] and the source function at the boundary, $s_b = s(0) = s(\tau^0)$, and at the center, $s_c = s(\frac{1}{2}\tau^0)$, of the plane parallel slab. Read: $5.9^{-2} = 5.9 \times 10^{-2}$.

	$\varepsilon_0 = 10^{-4}$					
τ^0	δ_0	η	s_b	s_c	$\frac{s_c - s_b}{s_c + s_b}$	$\frac{s_c}{s_b}$
10^2	0	4.6^{-3}	1.3^{-3}	1.1^{-2}	0.78	8.0
	0.01	4.6^{-3}	1.4^{-3}	1.1^{-2}	0.76	7.3
	0.1	4.5^{-3}	1.7^{-3}	1.0^{-2}	0.72	6.3
	1	4.5^{-3}	2.2^{-3}	1.0^{-2}	0.64	4.5
	10	4.5^{-3}	3.4^{-3}	7.6^{-3}	0.37	2.2
	100	4.4^{-3}	4.2^{-3}	5.0^{-3}	0.08	1.2
10^4	0	0.12	8.5^{-3}	0.66	0.98	79
	0.01	0.12	9.3^{-3}	0.67	0.97	72
	0.1	0.12	1.1^{-2}	0.67	0.97	63
	1	0.12	1.5^{-2}	0.67	0.96	45
	10	0.12	2.8^{-2}	0.67	0.92	24
	100	0.13	6.1^{-2}	0.66	0.83	11
10^6	0	0.29	9.5^{-3}	0.99	0.98	105
	0.01	0.29	1.0^{-2}	0.99	0.98	95
	0.1	0.29	1.2^{-2}	0.99	0.98	83
	1	0.29	1.6^{-2}	0.99	0.97	60
	10	0.29	3.1^{-2}	1.00	0.94	32
	100	0.30	6.8^{-2}	1.00	0.87	15

Table 3. Ratio of the maximum value of the emerging intensity, i_{max}^{out}, to the intensity at the line center, i_0^{out}. The frequencies x_{max} for which i_x^{out} assumes its maximum value i_{max}^{out} are, in general, different for different combinations of ε_0 and τ^0, but, for a given pair ε_0, τ^0, almost independent of δ_0 (see Figs. 3 and 4).

	i_{max}^{out}/i_0^{out}					
	$\varepsilon_0 = 10^{-2}$			$\varepsilon_0 = 10^{-4}$		
δ_0	$\tau^0 = 10$	10^2	10^3	$\tau^0 = 10^2$	10^4	10^6
0	1.04	2.5	4.4	2.8	29	52
0.01	1.04	2.5	4.4	2.8	29	52
0.1	1.03	2.4	4.3	2.7	28	51
1	1.01	2.2	3.9	2.4	26	46
10	1.00	1.5	2.7	1.5	16	30
100	1.00	1.1	1.6	1.1	7	14

so that these figures directly display the spatial distribution of excited atoms in the plane parallel slab, where the Planck function, $s = 1$, corresponds to the Boltzmann value of n_2/n_1. As expected, larger values of δ_0 give rise to flatter spatial distributions of excited atoms. This flattening with increasing values of δ_0 can readily be followed by considering the ratios $(s_c - s_b)/(s_c + s_b)$ and s_c/s_b, quoted in Tables 1 and 2, where s_c and s_b denote the values of the source functions at the center and at the boundary of the slab. Likewise, as a result of this flattening of the source function, the emitted

double-humped intensity profiles become flatter, as can be seen in Figs. 3 and 4, which show typical intensity profiles of effectively thin and effectively thick plasmas, as well as in Table 3, where we have listed the ratio of the maximum value of the emerging intensity i_x^{out} to its value at the line center, which is a measure of the self-reversal of the line.

At least for the range of parameters considered, the total radiative energy loss in the spectral line is hardly affected by diffusion of excited atoms, as shown by the values of the quantity η, Eq. (23), quoted in Tables 1 and 2.

As expected on physical grounds, the effect of diffusion is most important at the boundary of the plasma where higher values of δ_0 lead to higher values of the source function, reflecting the increasing convective transport of excited atoms from deeper layers into the boundary region. Even moderate values of δ_0 significantly change the boundary value of s. Roughly, the boundary value of s for $\delta_0 = 1$ is about twice as large as that for $\delta_0 = 0$ (see Tables 1 and 2). As a consequence, the intensity profile near the line center of the emitted spectral line depends rather sensitively on δ_0 (see Figs. 3 and 4). The dimension of the boundary region affected by particle diffusion increases with increasing δ_0. From Figs. 1 and 2 (and also from our other results not presented here graphically), it can be seen that this region extends from the boundary $\tau = 0$ to an optical depth $\tau \cong 1$ for $\delta_0 = 1$, to $\tau \cong 10 \cdots 30$ for $\delta_0 = 10$, and to $\tau \cong 10^2 \cdots 10^3$ for $\delta_0 = 100$. One therefore expects that, for sufficiently large values of the diffusion parameter, an otherwise effectively thick system becomes effectively thin.

In this paper, we have only considered the limiting case of pure Doppler broadening. It is well known [2] that additional collision broadening of the spectral line has the effect of decreasing the density gradients of excited atoms because more photons emitted at deeper layers escape from the system in the line wings. Thus, the diffusion effects found for pure Doppler broadening establish upper limits for the more general case of a line which shows combined Doppler and collision broadening. The case of combined Doppler and natural broadening is more involved since natural broadening, in contrast to collision broadening, is characterized by frequency coherence of the scattered photon in the rest frame of the atom. Finally, it should be remembered that our calculations refer only to the special case of a plasma with vanishing exchange of matter with the surroundings where the boundary conditions (12) hold.

Despite being somewhat unrealistic, two-level atoms, which were considered in this paper, serve useful purposes. Firstly, the radiation transport in strong resonance lines can often be described, at least approximately, as being due to two-level atoms. Secondly, the problem of radiative transfer in several interlocking lines can be treated by an iterative procedure where the source function of each line is considered as that of a two-level atom, with parameters depending on the radiation intensities in all other lines.

Appendix

Because of the symmetry of the system, the integro-differential equation (10) can be written in a form restricted to the interval $0 \leqq \tau \leqq \frac{1}{2}\tau^0$ with boundary conditions $s'(0) = s'(\frac{1}{2}\tau^0) = 0$. We have treated this equation in a straightforward manner simply by replacing derivatives there by differences and integrals by sums. The most crucial approximation made consisted in writing the integral as

$$\sum_{i=1}^{N} \int_{\Delta\tau_i} K_1(|\tau - \tau'|)\, s(\tau')\, \mathrm{d}\tau' \cong \sum_{i=1}^{N} s(\tau_i) \int_{\Delta\tau_i} K_1(|\tau - \tau'|)\, \mathrm{d}\tau',$$

where $\Delta\tau_i$ is a τ-interval containing the point τ_i. In this way one obtains from Eq. (10) a system of linear equations for the N unknowns $s_i = s(\tau_i)$. The maximum N used by us was about $N = 180$.

Owing to the approximation just mentioned, it was necessary to choose the intervals $\Delta\tau_i$ such that the relative change of s from one interval to the next was nearly constant over the entire τ-interval, i.e. that $\Delta s_i/s_i = [s(\tau_{i+1}) - s(\tau_i)]/s(\tau_i)$ was approximately independent of i. Applying this criterion, good numerical results were easily obtained if $\delta_0 \lesssim 1$. However, if $\delta_0 \gg 1$, it turned out that $\Delta s_i/s_i$ had to be constant for all i to a high accuracy, otherwise the results were unreliable. Therefore, starting from a more or less arbitrary initial choice of the $\Delta\tau_i$, we changed these intervals by an iterative procedure until $\Delta s_i/s_i$ was independent of i. This was then repeated for larger values of N in order to test the convergence with increasing N. The errors of the results thus obtained should not

exceed about 5% if $\delta_0 = 100$, and they are much smaller for smaller values of δ_0.

For very small ε_0, very large δ_0, and very large τ^0, however, other methods of solving the integro-differential equation (10) are required in order to get numerical stability. A possible candidate is the "kernel approximation" used by Avrett and Hummer [2]. Taking diffusion into account merely gives rise to an additional term $-\delta_0 k_\alpha^2$ on the left-hand side of the characteristic equation [Ref. [2], Eq. (4.4)], the second equation of the kernel approximation [Ref. [2], Eq. (4.5)] remaining unchanged.

[1] D. F. Düchs and J. Oxenius, Z. Naturforsch. **32a**, 156 (1977).

[2] E. H. Avrett and D. G. Hummer, Mon. Not. R. Astr. Soc. **130**, 295 (1965).